

Mid-to-high- Z precision x-ray measurements

E. G. Kessler, Jr., R. D. Deslattes, D. Girard,* W. Schwitz,[†] L. Jacobs,[‡] and O. Renner[§]
Quantum Metrology Group, National Bureau of Standards, Washington, D.C. 20234

(Received 13 April 1982)

New x-ray wavelength (energy) and width measurements are reported for a number of elements from $47 \leq Z \leq 92$. The x rays were produced with the use of an electron Van de Graaff, and the measurements were made with a two-axis flat-crystal transmission spectrometer equipped with angle-measuring interferometers. The new measurements reported here, combined with other high-precision x-ray wavelengths, form a moderately extensive data base for comparison with theoretical calculations. Comparison with recent revisions of a previously available all- Z calculation reveals improved patterns of general agreement with, however, important exceptions. The newly measured linewidths are in agreement with widths calculated via relativistic wave functions used for the term estimates.

I. INTRODUCTION

In an earlier paper¹ selected x-ray wavelengths were compared with then available all- Z relativistic self-consistent-field calculations and showed a suggestive pattern of inconsistency between theory and experiment. The experimental data used consisted of a very few new results from our own work combined with high-precision ratios otherwise available which could be used to expand the results and which were traceable in some manner to the optical wavelength scale. The differences ($E_{\text{expt}} - E_{\text{theor}}$) were found to have linear Z dependences with values of 7 eV around Z in 90 and 0 eV around $Z=20$ for the $K\alpha$ lines. These discrepancies led us to a program of precision x-ray measurements over a wide range of Z . Our goal was to generate sufficient new measurements to see if the above discrepancies would be confirmed and to seek possibly finer details not evident from the initial small-data set. In the best case, one might imagine that evidence of difficulty with a particular component of the theoretical estimate might emerge from such a study,

II. EXPERIMENTAL

Over the past ten years x-ray and γ -ray wavelength measurement capabilities having noticeably improved accuracies were established at the (U.S.) National Bureau of Standards (NBS). These capabilities depend on x-ray-optical interferometry for measurement of a crystal lattice spacing in terms of optical wavelengths, lattice spacing intercomparison facilities which measure the small differences between tokens of measured and used crystal samples, and double flat-crystal transmission spectrometers

which measure the (small) Bragg angles through which x and γ rays are diffracted. The Bragg-angle-measuring spectrometers depend for their high performance on use of angle-measuring interferometers having an accuracy of a few tenths of m arcsec. These procedures have been summarized in a recent review article.² The x-ray measurements reported here were made with a second generation double-crystal transmission spectrometer and use results of the x-ray-optical interferometry as well as the lattice-spacing intercomparison. The second generation differs from the instrument described in the review article in that it is configured to accommodate use of stationary sources, has a ± 15 -deg angular range, and is under computer control. The wavelengths (and energies) that are reported here are on a scale which is consistent with the optical wavelength scale and thereby with the scale used in theoretical calculation (e.g., R_{∞}^{-1}).

The double-crystal spectrometer was located in the target area of a 4-MeV electron Van de Graaff at NBS, Gaithersburg. The accelerator operated mostly at an electron energy of 2.5 MeV, a compromise between satisfactory operation of the Van de Graaff and photon yields. The electron beam entered a target chamber bombarding solid samples mechanically attached to a water-cooled Al target holder. The position and shape of the electron beam's focus on the samples were monitored using fluorescent coatings and a television camera. The beam was approximately circular with 2–3-mm diameter. An electrometer was used to measure the beam current and to normalize the x-ray intensity. For the measurements on Xe, a high-pressure (2×10^6 Pa) thin-window (0.5 mm) water-cooled gas cell was used.

The targets were made from samples with naturally occurring isotopic abundances and having moderate impurity levels (0.1 at. %). Sample thicknesses were chosen using the data of Ref. 3 to obtain >75% of the maximum possible yield. For materials with poor heat conductivity (e.g., Pb) an Al cover plate ~0.3-mm thick was used to prevent the sample from melting and vaporizing.

The flat crystals were Si wafers cut so that the 220 planes were used in symmetric Laue-case geometry. The efficiency of such a double-flat-crystal spectrometer is a few times 10^{-11} so that only strong x-ray lines can be accurately measured with a reasonable effort. Our measurements were thus restricted to the $K\alpha_1$, $K\alpha_2$, $K\beta_1$, and $K\beta_3$ transitions. The diffraction angles ranged from 8.4 deg for Ag to 1.9 deg for U.

During measurement the spectrometer was under computer control with interfacing via a CAMAC system. X-ray profiles were recorded in a point-by-point manner using a NaI (Tl) detector. The data recorded for each point included interferometer fringe number, crystal and instrument temperature, air pressure, air temperature, humidity, x-ray counts, and electron-beam current. A computer program corrected observed fringe numbers for atmospheric conditions and stored the pertinent information on a magnetic disk for off-line fitting. Profiles were recorded with the two crystals in the parallel (nondispersive) position and the two crystals in the antiparallel (dispersive) position. The counting time for each point ranged from 10 sec for intense parallel profiles to 100 sec for weak antiparallel profiles.

The width of the parallel position profile for a given energy is a measure of the instrumental width at that energy. The instrumental widths ranged from 1.8 sec at 22.2 keV (Ag $K\alpha_1$, $\theta_B = 8.4$ deg) to 0.77 sec at 98.4 keV (U $K\alpha_1$, $\theta_B = 1.9$ deg). The instrumental resolving power thus ranged from 17000 at 22 keV to 9000 at 98 keV. The antiparallel position profiles are a convolution of the x-ray line profile and the instrumental profile. The measured x-ray linewidths ranged from 8.6 eV at 22.2 keV to 103.8 eV at 98.4 keV. Thus, for example, to make wavelength measurements with an accuracy of ~5 ppm, the dispersive profiles had to be divided into a few hundred parts in a typical case.

III. DATA ANALYSIS

Data were transferred from local disks to the NBS central computing facility via phone line. The

profiles were there fitted to model functions using nonlinear least-squares criteria. The model for the parallel profiles was a Lorentzian function with an adjustable position, intensity, width, and background. Two models were used for the antiparallel position profiles. In previous measurements on γ rays, which have a smaller wavelength spread, a Lorentzian function convoluted with a vertical divergence function provided a good fit to the measured line shape.⁴ The parameters for the vertical divergence are known from the geometry of the source and Soller collimators. Such a model also provided a satisfactory fit to the x-ray data. As in the parallel position case, the position, intensity, width, and background were adjusted. In the case of x-ray lines, the vertical divergence function makes only a minor contribution to the composite profiles because the x-ray lines themselves have such large intrinsic widths. Approximately half of the dispersive profiles were also fit with just a Lorentzian function. The statistical incertitude of the data is such that the two models fit the recorded profiles equally well and return parameters which differ less than the measurement uncertainty (typically ~2 ppm). Plots of recorded profiles and the computer fits for U $K\alpha_1$ are shown in Fig. 1.

The differences in the $K\beta_1$ and $K\beta_3$ energies are small enough that the recorded $K\beta_1$ and $K\beta_3$ profiles are slightly overlapping. In order to account for the influence of this slight overlap, the recorded $K\beta$ data were fit with a two-component model which adjusted the parameters for the two components simultaneously.

In order to monitor the adequacy of our model profiles, the differences between the data and the computer fit were plotted and examined for systematic trends. Significant asymmetry in the profiles might, for example, signal the presence of (expected) satellite contributions which, as is well known, are sensitive to the physical and chemical state of the target. No asymmetry which could shift the profile peaks by more than the measurement uncertainty was noted in any of the profiles, thereby establishing limiting values for the influence of multivacancy processes (typically less than 2 ppm).

IV. EXPERIMENTAL RESULTS

Table I indicates the elements and their characteristic wavelengths which were measured. ($K\beta$ lines were not measured for all the elements.) The elements listed were chosen for their availability,

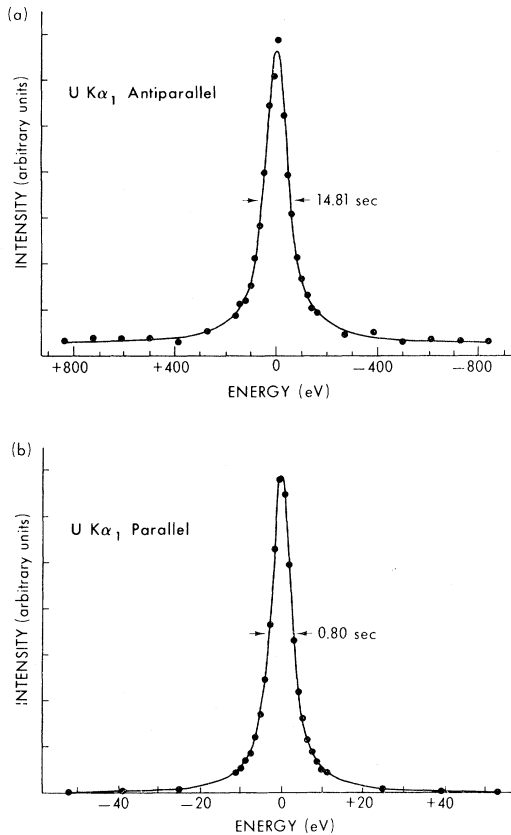


FIG. 1. (a) Antiparallel and (b) parallel profiles for U K α_1 . Dots are the recorded points and the line is the computer fit of the profile. Horizontal scale for the parallel profile is ~ 18.5 times smaller than that for the antiparallel profile.

ease of handling, and their position in the Periodic Table. Energies were obtained from observed wavelengths using the most recently recommended energy-wavelength conversion factor $V\lambda = 1.239\,8520 \times 10^{-6}$ eV m, which, for the present purpose, is taken (as a convention) to hold without error.⁵ This conversion factor carries, however, an additional uncertainty of 2.6 ppm, which, though not important in the present study, may affect certain applications of these results. The uncertainties indicated represent estimated standard deviations of the mean derived from 10 to 16 individual measurements of each wavelength.

It is appropriate to compare these new measurements with other measurements involving these same lines as summarized in the wavelength table of Bearden.⁶ Since the wavelength values in this table are given in the A^* scale, they were corrected by the conversion factor $1.000\,0167 \text{ \AA}/A^*$ [0.9 ppm (Ref.

7)] and converted to energies using the above $V\lambda$ product. The differences between the new measurements and the Bearden summary are presented in Table II along with the combined uncertainties. The differences range from several tenths of an eV in the $Z=55$ region to more than 10 eV in the $Z=90$ region and, in some cases, exceed three times the combined uncertainties. There are no obvious patterns either for a given transition as a function of Z or for a fixed Z as a function of transition. At high Z the new results are four or more times more accurate than those summarized by Bearden⁶ and, as is shown below, comparisons of the new results with recent theoretical calculations show smooth trends at high Z , while comparisons using the results summarized by Bearden do not. These two observations suggest that the values in Bearden's tables should be used with caution in the region of high Z .

In Table III other recent precision x-ray measurements are compared with those reported here. All of these results were obtained with precision curved-crystal spectrometers. Since the measurements from Ref. 9 were made relative to the previously accepted value of the ^{198}Au 411-keV line, they have been corrected for the new value for this line.⁴ In Ref. 11 small differences between x-ray lines in different orders were measured. Of the differences reported only the U K β_1 in second order and the Er K β_1 in first order can be compared to our results. The Er K β_1 energy given above was used along with the measured energy difference to obtain the U K β_1 result. In almost all cases, the values obtained in this study are smaller than those reported by other experimenters with differences less than two standard deviations in most cases. The precision high- Z measurements presented in Table III are in much better agreement with our new measurements than the earlier compiled data.

V. DATA SET FOR THEORETICAL COMPARISON

In order to make an experiment versus theory comparison over as large a range of Z as possible, the above data were augmented by a selection of measurements from other sources which (1) could be placed on the same energy scale, and (2) had an accuracy comparable to the above results. All the data included had an uncertainty < 25 ppm except for a few measurements at very high Z . We naturally include also those x-ray lines which had been previously measured using techniques similar to

TABLE I. Experimental measurements.

Z	Element	X-ray line	Wavelength (pm)	Uncertainty (ppm)	Energy (eV)	Width (eV)
47	Ag	$K\alpha_2$	56.381 42	4.7	21 990.44	8.9±0.8
		$K\alpha_1$	55.942 27	1.3	22 163.06	8.6±0.4
54	Xe	$K\alpha_2$	42.088 18	1.8	29 458.44	14.5±1.0
		$K\alpha_1$	41.635 16	3.2	29 778.97	14.3±0.9
		$K\beta_3$	36.940 58	3.6	33 563.42	17.3±3.4
		$K\beta_1$	36.873 53	3.6	33 624.45	16.6±2.2
56	Ba	$K\alpha_2$	38.968 45	2.0	31 816.82	16.3±1.0
		$K\alpha_1$	38.512 53	2.2	32 193.47	16.5±0.5
		$K\beta_3$	34.152 34	3.2	36 303.58	17.0±1.4
		$K\beta_1$	34.082 77	2.1	36 377.68	18.4±1.2
60	Nd	$K\alpha_2$	33.647 98	2.1	36 847.74	20.6±0.9
		$K\alpha_1$	33.185 75	1.9	37 360.98	20.5±0.5
62	Sm	$K\alpha_2$	31.369 88	2.5	39 523.64	24.1±0.9
		$K\alpha_1$	30.904 56	1.4	40 118.74	23.3±0.6
68	Er	$K\alpha_2$	25.711 377	4.1	48 221.92	32.9±2.0
		$K\alpha_1$	25.237 403	2.4	49 127.56	32.7±1.6
		$K\beta_3$	22.347 699	6.3	55 480.08	37.3±3.0
		$K\beta_1$	22.269 904	3.3	55 673.88	37.2±1.4
79	Au	$K\alpha_2$	18.507 695	3.3	66 991.16	59.2±3.7
		$K\alpha_1$	18.019 811	2.6	68 804.94	57.5±0.7
		$K\beta_3$	15.982 518	7.9	77 575.51	67.0±6.4
		$K\beta_1$	15.899 555	4.9	77 980.30	57.4±2.0
82	Pb	$K\alpha_2$	17.029 555	3.3	72 805.89	65.6±2.9
		$K\alpha_1$	16.537 845	2.3	74 970.59	66.3±1.9
		$K\beta_3$	14.681 320	7.1	84 450.99	70.3±6.8
		$K\beta_1$	14.596 861	4.0	84 939.63	67.8±4.0
90	Th	$K\alpha_2$	13.782 624	2.2	89 957.62	95.7±4.7
		$K\alpha_1$	13.282 044	2.7	93 347.98	93.8±3.2
		$K\beta_3$	11.828 707	6.6	104 817.21	100.5±8.8
		$K\beta_1$	11.740 779	5.0	105 602.19	94.6±4.1
92	U	$K\alpha_2$	13.099 133	5.9	94 651.45	106.3±6.1
		$K\alpha_1$	12.595 999	2.8	98 432.21	103.9±2.4
		$K\beta_3$	11.228 878	5.9	110 416.38	108.3±7.3
		$K\beta_1$	11.140 151	5.8	111 295.80	103.0±4.9

those employed for this study, e.g., $\text{Cu}K\alpha_1$, $\text{Mo}K\alpha_1$,^{7,12} and $\text{W}K\alpha_1$.⁷

In expanding the flat-crystal data set, we made particular use of curved-crystal spectrometer measurements on high-Z elements by Borchert⁹ and Barreau *et al.*¹⁰ Borchert gave results on Tm, Th,

U, and Pu, while Barreau *et al.* provided data for Ra, Ac, Th, Pa, Cm, and Bk. Although curved- and flat-crystal values for Th and U could have been averaged to obtain "best values," in this study we have chosen to use the high-precision flat-crystal data wherever available. Thus from Ref. 9 we ex-

TABLE II. Comparison of results with compiled data.

Element	$K\alpha_1$	σ	$E_{\text{Bearden}} - E_{\text{NBS}}$ (eV)		$K\beta_1$	σ	$K\beta_3$	σ
			$K\alpha_2$	σ				
Ag	0.23	0.05	0.26	0.25				
Xe	0.33	2.12	0.33	2.07	0.83	2.72	-0.94	2.71
Ba	0.66	0.50	0.82	0.61	1.18	0.55	1.14	0.69
Nd	0.67	0.34	0.24	0.34				
Sm	0.06	0.39	-0.56	0.39				
Er	0.94	0.59	-0.10	0.59	8.83	7.40	15.71	7.35
Au	0.04	1.15	-0.41	1.09	5.35	2.21	6.07	1.56
Pb	-0.14	1.36	-0.55	1.29	-2.23	5.18	0.43	3.46
Th	3.67	2.10	-3.30	1.94	8.84	12.00	15.15	4.00
U	8.51	3.48	15.28	4.32	5.64	7.42	-8.94	5.86

tracted values for $\text{Tm}K\alpha_{1,2}$, $\text{Tm}K\beta_1$, and $\text{Pu}K\alpha_{1,2}$, while Ref. 10 yielded data for $\text{Pa}K\alpha_{1,2}$, $\text{Cm}K\alpha_{1,2}$, $\text{Cm}K\beta_{1,3}$, and $\text{Bk}K\alpha_{1,2}$. Results on Ra and Ac are not included because their uncertainty is so large (more than 140 ppm) that they would add little to the comparison.

In order to expand the data for $Z < 50$ we use ratio measurements by Bearden and collaborators. The results of interest are wavelength ratios among the $K\alpha_{1,2}$ lines of Cr, Cu, Mo, Ag, and W having a precision of < 2 ppm.¹³ Wherever there has been opportunity to compare these ratios with more recent data,⁷ the agreement has been very satisfactory except for ratios involving W. Further measurements by Bearden¹⁴ appear to confirm that the reported W ratios are in error. In addition to the above-mentioned ratios, Bearden reported K -series measurements having a precision of 9 ppm for $44 \leq Z \leq 51$ in which $\text{Ag}K\alpha_1$ was used as standard.⁶

Using our flat-crystal value for $\text{Ag}K\alpha_1$, K -series wavelengths for elements with $44 \leq Z \leq 51$ are available which meet the conditions set forth at the beginning of this section. For purposes of illustration only results for $Z=44$ and $Z=51$ have been included. Finally a value for $\text{Al}K\alpha_1$ can be obtained by combining the ratio of $\text{Al}K\alpha_1$ to $\text{Cu}K\alpha_1$ reported by Henins¹⁵ and the $\text{Cu}K\alpha_1$ wavelength.^{7,12}

In a number of cases only $K\alpha_1$ or $K\alpha_{1,2}$ lines are available directly. In order to get needed values for $K\alpha_2$ and $K\beta_{1,3}$, it was assumed that the ratios $K\alpha_1/K\alpha_2$, $K\alpha_1/K\beta_1$, and $K\alpha_1/K\beta_3$ which can be extracted from Ref. 6 are valid. As Table II suggests, this assumption is probably valid for $Z \leq 60$. For $Z \leq 30$, no values for $K\beta_{1,3}$ were derived because only unresolved values for $K\beta$ are reported in Ref. 6. The expanded data set including energy values from Table I is presented in Table IV.

A number of measurements employing conver-

TABLE III. Comparison of results with other measurements.

Element	X-ray line	Reference	Energy (eV)	Uncertainty (eV)	Difference (eV)
Pb	$K\alpha_2$	8	72807.7	1.0	1.8 ± 1.0
Pb	$K\alpha_1$	8	74972.0	1.0	1.4 ± 1.0
Th	$K\alpha_2$	9	89957.5	0.7	0.1 ± 0.7
		10	89957	2	-0.6 ± 2
Th	$K\alpha_1$	9	93348.3	0.6	0.3 ± 0.7
		10	93348	2	0.0 ± 2
U	$K\alpha_2$	9	94653.0	0.8	1.5 ± 1.0
U	$K\alpha_1$	9	98434.1	0.7	1.8 ± 0.8
U	$K\alpha_1$	11	111300.8	1.0	5.0 ± 1.8

TABLE IV. Comparison of experimental and theoretical energies.

Z	Element	X-ray line	Experimental energy (eV)	Uncertainty (ppm)	Theoretical energy (eV)	Energy difference Expt-theor (eV)
13	Al	$K\alpha_2$	1 486.269	21.8	1 486.831	-0.562
		$K\alpha_1$	1 486.695	4.3	1 487.603	-0.908
24	Cr	$K\alpha_2$	5 405.565	1.9	5 404.428	1.137
		$K\alpha_1$	5 414.787	13.2	5 414.517	0.270
29	Cu	$K\alpha_2$	8 027.917	2.9	8 027.247	0.670
		$K\alpha_1$	8 047.865	1.0	8 047.379	0.486
42	Mo	$K\alpha_2$	17 374.40	12.7	17 372.944	1.456
		$K\alpha_1$	17 479.485	0.6	17 478.349	1.136
		$K\beta_3$	19 590.37	21.2	19 585.442	4.928
		$K\beta_1$	19 608.47	21.2	19 603.422	5.048
44	Ru	$K\alpha_2$	19 150.61	9.2	19 149.043	1.637
		$K\alpha_1$	19 279.29	9.3	19 278.387	0.973
		$K\beta_3$	21 634.79	10.4	21 630.867	3.923
		$K\beta_1$	21 656.89	10.4	21 653.495	3.395
47	Ag	$K\alpha_2$	21 990.44	4.7	21 988.933	1.503
		$K\alpha_1$	22 163.06	1.3	22 161.816	1.245
		$K\beta_3$	24 911.71	12.1	24 907.756	3.954
		$K\beta_1$	24 942.58	12.1	24 939.029	3.551
51	Sb	$K\alpha_2$	26 110.95	9.4	26 108.914	2.126
		$K\alpha_1$	26 359.03	9.5	26 357.399	1.731
		$K\beta_3$	29 679.40	14.2	29 674.737	4.663
		$K\beta_1$	29 725.72	10.7	29 721.763	3.957
54	Xe	$K\alpha_2$	29 458.44	1.8	29 456.681	1.756
		$K\alpha_1$	29 778.97	3.2	29 777.017	1.952
		$K\beta_3$	33 563.42	3.6	33 558.143	5.277
		$K\beta_1$	33 624.45	3.6	33 620.336	4.114
56	Ba	$K\alpha_2$	31 816.82	2.0	31 814.663	2.153
		$K\alpha_1$	32 193.47	2.2	32 191.442	2.030
		$K\beta_3$	36 303.58	3.2	36 298.273	5.307
		$K\beta_1$	36 377.68	2.1	36 372.657	5.032
60	Nd	$K\alpha_2$	36 847.74	2.1	36 846.072	1.671
		$K\alpha_1$	37 360.98	1.9	37 359.733	1.247
		$K\beta_3$	42 166.51	17.6	42 162.385	4.125
		$K\beta_1$	42 271.17	13.6	42 267.983	3.187
62	Sm	$K\alpha_2$	39 523.64	2.5	39 522.095	1.547
		$K\alpha_1$	40 118.74	1.4	40 117.714	1.021
68	Er	$K\alpha_2$	48 221.92	4.1	48 220.490	1.431
		$K\alpha_1$	49 127.56	2.4	49 126.606	0.953
		$K\beta_3$	55 480.08	6.3	55 474.793	5.287
		$K\beta_1$	55 673.88	3.3	55 668.724	5.156
69	Tm	$K\alpha_2$	49 772.99	2.4	49 771.402	1.588
		$K\alpha_1$	50 741.81	1.8	50 740.143	1.667
		$K\beta_1$	57 509.14	2.6	57 503.265	5.875

TABLE IV. (Continued.)

Z	Element	X-ray line	Experimental energy (eV)	Uncertainty (ppm)	Theoretical energy (eV)	Energy difference Expt-theor (eV)
74	W	$K\alpha_2$	57 982.64	13.9	57 979.826	2.814
		$K\alpha_1$	59 319.23	0.9	59 317.069	2.164
		$K\beta_3$	66 952.40	16.0	66 943.930	8.470
		$K\beta_1$	67 245.45	16.1	67 237.148	8.302
79	Au	$K\alpha_2$	66 991.16	3.3	66 988.486	2.676
		$K\alpha_1$	68 804.94	2.6	68 802.663	2.277
		$K\beta_3$	77 575.51	7.9	77 565.466	10.044
		$K\beta_1$	77 980.30	4.9	77 970.912	9.388
82	Pb	$K\alpha_2$	72 805.89	3.3	72 802.822	3.072
		$K\alpha_1$	74 970.59	2.3	74 966.587	4.004
		$K\beta_3$	84 450.99	7.1	84 439.731	11.259
		$K\beta_1$	84 939.63	4.0	84 928.489	11.141
90	Th	$K\alpha_2$	89 957.62	2.2	89 957.131	0.484
		$K\alpha_1$	93 347.98	2.7	93 348.838	-0.859
		$K\beta_3$	104 817.21	6.6	104 807.766	9.444
		$K\beta_1$	105 602.19	5.0	105 593.445	8.745
91	Pa	$K\alpha_2$	92 286	32.5	92 285.169	0.8
		$K\alpha_1$	95 863	31.3	95 866.833	-3.8
92	U	$K\alpha_2$	94 651.45	5.9	94 653.331	-1.879
		$K\alpha_1$	98 432.21	2.8	98 434.224	-2.013
		$K\beta_3$	110 416.38	5.9	110 407.725	8.655
		$K\beta_1$	111 295.80	5.8	111 288.879	6.921
94	Pu	$K\alpha_2$	99 523.8	12.1	99 525.850	-2.1
		$K\alpha_1$	103 734.7	5.8	103 735.317	-0.6
96	Cm	$K\alpha_2$	104 591	19.1	104 582.751	8.2
		$K\alpha_1$	109 273	18.3	109 263.844	9.2
		$K\beta_3$	122 303	16.4	122 281.336	21.7
		$K\beta_1$	123 404	16.2	123 384.565	19.4
97	Bk	$K\alpha_2$	107 181	56.0	107 185.021	-4.0
		$K\alpha_1$	112 130	26.8	112 119.933	10.1

sion electron spectrometers and/or Ge (Li) detectors have been made on elements having $Z \geq 95$. These measurements are noted in a 1977 comparison of experimental and theoretical values.¹⁶ We have not included these measurements in our expanded data set because the uncertainties are large (~ 100 ppm), and the calibrations of the spectrometers are not clearly related to the energy scale used in the theoretical calculations.

VI. THEORETICAL COMPARISON— TRANSITION ENERGIES

In Table IV, theoretical transition energies from Huang *et al.*¹⁷ as subsequently revised by Chen *et al.*¹⁸ are listed for all the lines. The basic calculation used relativistic Hartree-Fock-Slater wave functions and assumed complete relaxation, first-order correction to the local approximation, and

quantum-electrodynamic corrections. The recent revision of this calculation by Chen *et al.*¹⁸ employs a more realistic nuclear charge distribution, a more accurate expression for the Breit interaction, and a screened self-energy correction. Although Ref. 18 is limited to the K and L levels for $Z \geq 70$, Chen and Crasemann have kindly provided us with K and L energies for several elements with $50 \leq Z \leq 68$.¹⁹ By interpolation and extrapolation, theoretical estimates for $K\alpha_{1,2}$ lines for all Z listed in Table IV were obtained. The main effect of this important revision of the calculation of Ref. 17 has been to eliminate the dominant Z -dependent trend which was previously reported.¹ This can be seen in the graphical presentation of the comparisons in Fig. 2 for the $K\alpha$ lines, which shows more or less constant differences of 1–2 eV up to $Z \sim 85$, differences near zero around $Z=90$, negative differences in the $92 < Z < 95$ range, and larger (5-eV) positive differences in the $Z=97$ range.

Since revised calculations for the M levels are not yet available, theoretical transition estimates for $K\beta_1$ and $K\beta_3$ were obtained by combining the revised K binding energies and the M_{II} and M_{III} bind-

ing energies from Huang *et al.*¹⁷ and are listed in Table IV. Figure 3 shows the differences between experimental and theoretical transition energies for the $K\beta$ lines. Although the differences are significantly reduced over those obtained when the earlier theoretical calculations are used, there is still a discrepancy which increases with Z reaching ~ 10 eV at $Z=85$ and decreasing to ~ 7 eV in the $Z=90$ region. Since the K -level energies are common to the $K\alpha$ and $K\beta$ transitions, the remaining discrepancies for the $K\beta$ lines appear to be associated with the M levels.

For both $K\alpha$ and $K\beta$ transitions, the region of $Z > 90$ is particularly interesting because of the apparently large changes in the experiment-theory difference and the high values of $Z\alpha$. More and better experimental measurements in this region are needed and are planned.

It is surely questionable to compare, as we have done here, results of atomic calculations with data obtained predominantly from solid samples.

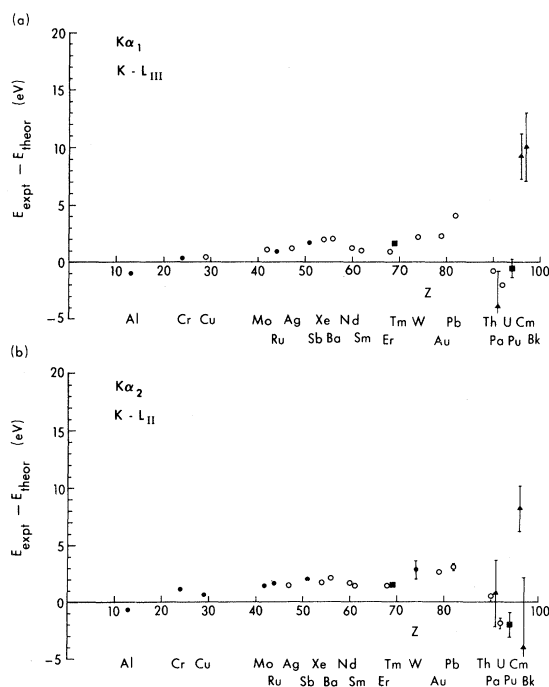


FIG. 2. Energy differences between experimental values and theoretical estimates of Chen *et al.* (Refs. 18 and 19) for $K\alpha_1$ (a) and $K\alpha_2$ (b) emission lines as a function of Z . The symbols are ●, Ref. 6; ○, this work; ■, Ref. 9; ▲, Ref. 10.

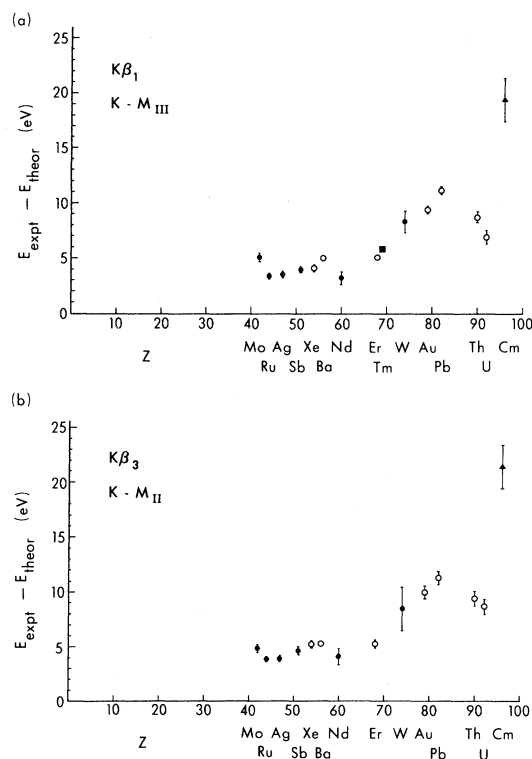


FIG. 3. Energy differences between experimental values and theoretical estimates of Chen *et al.* (Refs. 18 and 19) and Huang *et al.* (Ref. 17) for (a) $K\beta_1$ and (b) $K\beta_3$ emission lines as a function of Z . See text for explanation of theoretical estimates. The symbols are ●, Ref. 6; ○, this work; ■, Ref. 9; ▲, Ref. 10.

A priori, one can surmise that two sufficiently deep vacancies may experience equal chemical and solid-state perturbations thereby justifying such comparisons. Perhaps even more persuasive in this regard is the inclusion of data from gaseous Xe in the tables and figures. It appears in no way distinguished, thereby lending credence to the above drastic assumption.

VII. THEORETICAL COMPARISON WIDTHS

The widths presented in Table I are values for the full widths at half maximum of the x-ray lines. They were obtained from the recorded profiles by removing the instrumental contribution. The uncertainties in the widths were derived from the variation in the width parameter determined by the profile-fitting program. The average uncertainty in the widths is about 5%.

In Table V, the measured widths for $K\alpha_1$ and $K\alpha_2$ are compared with recent relativistic theoretic

calculations by Chen *et al.*²⁰ and widths measured by Nelson and Saunders²¹ using a bent-crystal spectrometer. Except for $NdK\alpha_1$, our width measurements agree with the results of Refs. 20 and 21 within the stated uncertainty. Figure 4, in which the differences between the experimental measurements and those of Ref. 20 are plotted, shows that our results are in excellent agreement with theoretical line widths and exhibit smaller fluctuations than the data of Ref. 21. The measured widths for $K\alpha_1$ and $K\alpha_2$ are also in excellent agreement with the semiempirical natural linewidths of Krause and Oliver.²²

Nearly degenerate satellite lines are well known in x-ray spectra and may make a significant contribution to the width. In some cases, precision wavelength measurements have been corrected for their presence on the basis of a model calculation.²³ Such satellites are also known to be sensitive to the physical and chemical state of the emitting atom. Since observed linewidths for all Z (including those of Xe) show no evidence of contributions from satellite

TABLE V. Comparison of experimental and theoretical widths.

Z	Element	X-ray line	NBS	Width (eV)	
				Ref. 20	Ref. 21
47	Ag	$K\alpha_2$	8.9 ± 0.8	9.08	
		$K\alpha_1$	8.6 ± 0.4	8.91	
54	Xe	$K\alpha_2$	14.5 ± 1.0	14.54	
		$K\alpha_1$	14.3 ± 0.9	14.31	
56	Ba	$K\alpha_2$	16.3 ± 1.0	16.51	18.0 ± 2.7
		$K\alpha_1$	16.5 ± 0.5	16.27	15.2 ± 0.9
60	Nd	$K\alpha_2$	20.6 ± 0.9	20.91	21.2 ± 3.2
		$K\alpha_1$	20.5 ± 0.5	20.71	14.4 ± 0.9
62	Sm	$K\alpha_2$	24.1 ± 0.9	23.39	24.2 ± 3.6
		$K\alpha_1$	23.3 ± 0.6	23.23	23.9 ± 1.4
68	Er	$K\alpha_2$	32.9 ± 2.0	32.57	29.5 ± 4.4
		$K\alpha_1$	32.7 ± 1.6	32.48	
79	Au	$K\alpha_2$	59.2 ± 3.7	57.51	56.7 ± 8.5
		$K\alpha_1$	57.5 ± 0.7	57.53	55.5 ± 3.3
82	Pb	$K\alpha_2$	65.6 ± 2.9	66.33	68.7 ± 10.3
		$K\alpha_1$	66.3 ± 1.9	66.38	65.5 ± 3.9
90	Th	$K\alpha_2$	95.7 ± 4.7	95.91	92.6 ± 13.9
		$K\alpha_1$	93.8 ± 3.2	95.94	95.0 ± 5.7
92	U	$K\alpha_2$	106.3 ± 6.1	104.93	107.5 ± 16.1
		$K\alpha_1$	103.9 ± 2.4	104.51	105.0 ± 6.3

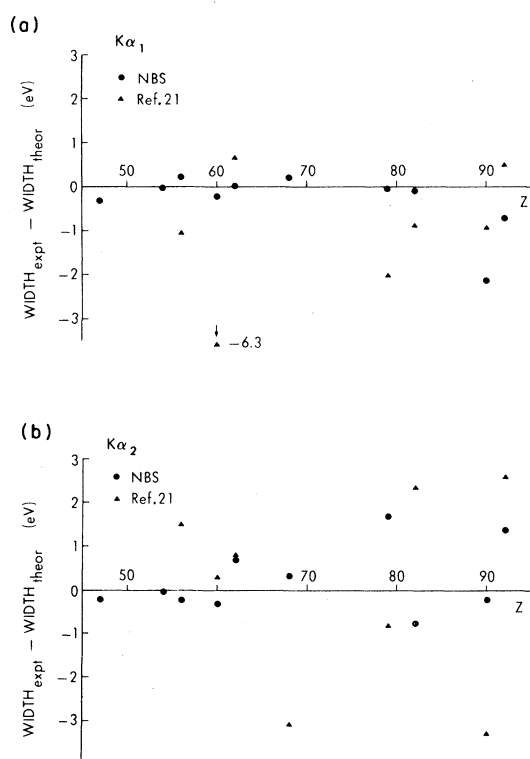


FIG. 4. Differences of natural linewidths between experimental values and relativistic theoretical estimates of Chen *et al.* (Ref. 20) for (a) $K\alpha_1$ and (b) $K\alpha_2$ emission lines as a function of Z . The symbols are ●, this work; ▲, Ref. 21.

lines, this complication has been neglected in this study. The lack of asymmetry of the recorded profiles noted earlier also supports neglecting satellite contributions.

VIII. DISCUSSION

We focus here on what appear to be the systematics of transition energy comparisons. These are emphasized in preference to term energies because of their relative insensitivity to chemical and solid-state effects as mentioned above. Such an approach entails the obvious disadvantage that energy levels are then only seen pairwise so that unique conclusions would appear difficult to extract. On the other hand, we can generally look at groups of transitions sharing an initial- or final-state configuration. Although complex, one can readily see a procedure evolving in which carefully drawn comparisons do yield informative guidance for the further development of our present understanding.

More specifically, one notes the relatively constant 1–2 eV discrepancies for $K\alpha_1$ and $K\alpha_2$ over a fairly wide range in Z (see Fig. 2). It has been suggested²⁴ that such an offset is to be expected from uncalculated effects of electron correlations. For inner levels ground-state and hole-state configuration interaction with nearby bound states and with radiation and radiationless continua may have to be considered.

Although the $K\beta$ energies have not been properly revised, preliminary calculations by Chen²⁵ suggest that in the region of $Z=90$, the M levels will shift in a manner to decrease the discrepancy by ~ 2 eV. Thus the conspicuous feature of Figs. 2 and 3, a discrepancy significantly larger for the $K\beta$ lines than the $K\alpha$ lines, is likely to remain even when the revisions indicated above are made. This is at first surprising since it might be thought that M -shell electrons would suffer less from quantum-electrodynamic corrections and their corresponding uncertainties. There is, however, an additional perturbing mechanism whose effects lean in the contrary direction. What is involved is coupling of inner vacancy levels to degenerate (Auger) decay continua. Here one expects to see, in general, changes in widths and shifts, also. Coupling of the $M_{II,III}$ levels to continua is expected to be larger than for the $L_{II,III}$ levels.

An informative discussion of the problem with particular application to $Kr 3p^{-1}$ was presented by Ohno and Wendin.²⁶ There it was found that shifts in the $3p$ levels with values between 2.6 and 3.0 eV were to be expected. For higher values of Z , this shift is expected to increase with Z but not very rapidly. Preliminary estimates by Chen²⁵ of shifts in the M levels resulting from coupling to decay continua in the region of $Z=90$ are on the order of 6 eV. Comparison of the differences between $K\beta$ and $K\alpha$ discrepancies show a pattern consistent with the assumption that such a continuum coupling mechanism is operative. However, until quantitative estimates become available, this conclusion should be regarded as tentative.

ACKNOWLEDGMENTS

The assistance of Dr. Charles Dick and Mr. John Mills of the Center for Radiation Research in the operation and maintenance of the Van de Graaff facility is gratefully acknowledged. We thank B. Crasemann and M. H. Chen for providing unpublished and preliminary calculations and many helpful discussions.

- *Laboratoire de Physique Atomique et Nucléaire, Université Pierre et Marie Curie, Paris, France.
- †University of Fribourg and Swiss National Science Foundation.
- ‡IKS Leuven University/SCK, Mol, Belgium.
- §Institute of Physics, Czech. Acad. Sci., Prague, Czechoslovakia.
- ¹R. D. Deslattes, E. G. Kessler, Jr., L. Jacobs, and W. Schwitz, *Phys. Lett.* **71A**, 411 (1979).
- ²R. D. Deslattes, E. G. Kessler, W. C. Sauder, and A. Henins, *Ann. Phys. (N.Y.)* **129**, 378 (1980).
- ³C. E. Dick, A. C. Lucas, J. M. Motz, R. C. Placious, and J. H. Sparrow, *J. Appl. Phys.* **44**, 815 (1973).
- ⁴E. G. Kessler, Jr., R. D. Deslattes, A. Henins, and W. C. Sauder, *Phys. Rev. Lett.* **40**, 171 (1978).
- ⁵E. R. Cohen and B. N. Taylor, *J. Phys. Chem. Ref. Data* **2**, 663 (1973).
- ⁶J. A. Bearden, *Rev. Mod. Phys.* **39**, 78 (1967). The quoted uncertainties which are probable errors (50% confidence limits) were expanded by 1.48 to obtain standard deviation errors (67% confidence limits). This error expansion factor assumes that the errors display a Gaussian distribution.
- ⁷E. G. Kessler, Jr., R. D. Deslattes, and A. Henins, *Phys. Rev. A* **19**, 215 (1979).
- ⁸P. Hungerford, H. H. Schmidt, R. Brissot, G. Barreau, and H. G. Börner, *Z. Naturforsch.* **36a**, 919 (1981).
- ⁹G. L. Borchert, *Z. Naturforsch.* **31a**, 102 (1976).
- ¹⁰G. Barreau, H. G. Börner, W. F. Davidson, R. W. Hoff, P. Jeuch, J. Larysz, K. Schreckenbach, T. von Egidy, and D. H. White, in *Proceedings of the Third International Symposium on Neutron Capture Gamma-ray Spectroscopy and Related Topics*, edited by R. E. Chrien and W. R. Kane (Plenum, New York, 1979), p. 552.
- ¹¹G. L. Borchert, P. G. Hansen, B. Janson, H. L. Ravn, and J. P. Desclaux, in *Atomic Masses and Fundamental Constants 6*, edited by J. A. Nolen, Jr. and W. Benenson (Plenum, New York, 1980), p. 189.
- ¹²R. D. Deslattes and A. Henins, *Phys. Rev. Lett.* **31**, 972 (1973). Wavelengths in this reference were corrected as explained in Ref. 7.
- ¹³J. A. Bearden, A. Henins, J. G. Marzolf, W. C. Sauder, and J. S. Thomsen, *Phys. Rev.* **135**, A899 (1964).
- ¹⁴J. A. Bearden (private communication).
- ¹⁵A. Henins, *Precision Measurements and Fundamental Constants*, Natl. Bur. Stand. (U.S.), Spec. Publ. No. 343 (U. S. GPO, Washington, D.C., 1971), p. 255.
- ¹⁶M. O. Krause and C. W. Nestor, Jr., *Phys. Scr.* **16**, 285 (1977).
- ¹⁷K.-N. Huang, M. Aoyagi, M. H. Chen, B. Crasemann, and H. Mark, *At. Data Nucl. Data Tables* **18**, 243 (1976).
- ¹⁸M. H. Chen, B. Crasemann, M. Aoyagi, K.-N. Huang, and H. Mark, *At. Data Nucl. Data Tables* **26**, 561 (1981).
- ¹⁹M. H. Chen and B. Crasemann (private communication). Binding energies for the K , L_2 , and L_3 levels for $Z=50, 53, 55, 57, 60, 63, 65$, and 68 were provided. Because a uniform charge distribution for the nucleus was used, the values provided were corrected a small amount using Ref. 18, Fig. 1 to account for a Fermi distribution of the nuclear charge.
- ²⁰M. H. Chen, B. Crasemann, and H. Mark, *Phys. Rev. A* **21**, 436 (1980); **24**, 177 (1981). For elements which were not explicitly tabulated in these articles, widths were estimated by graphical interpolation.
- ²¹G. C. Nelson and B. G. Saunders, *J. Phys. (Paris) Colloq. Suppl.* **10** **32**, C4-97 (1971).
- ²²M. O. Krause and J. H. Oliver, *J. Phys. Chem. Ref. Data* **8**, 329 (1979).
- ²³G. L. Borchert, P. G. Hansen, B. Janson, I. Lindgren, H. L. Ravn, O. W. B. Schult, and P. Tedemond-Petersson, *Phys. Lett.* **65A**, 297 (1978).
- ²⁴M. H. Chen, B. Crasemann, and H. Mark, *Phys. Rev. A* **24**, 1158 (1981).
- ²⁵M. H. Chen (private communication of preliminary results).
- ²⁶M. Ohno and G. Wendin, *Phys. Scr.* **16**, 299 (1977).